DAFS Study of Local Structure of Ordered Nanodomains in $PbMg_{1/3}Nb_{2/3}O_3$

A. I. Frenkel,[*] D. M. Fanning,[†] I. K. Robinson,[*,†] D. L. Adler,[‡] and J. O. Cross[§]

[*] *Materials Research Laboratory,*[1]
University of Illinois at Urbana - Champaign, Urbana, Illinois 61801
[†] *Loomis Laboratory, Physics Department*
University of Illinois at Urbana - Champaign, Urbana, Illinois 61801
[‡] *KLA Instruments Corp., San Jose, California*
[§] *Naval Research Laboratory,*[2] *Washington, D.C. 20375.*

Abstract.
We have performed a Diffraction Anomalous Fine Structure (DAFS) study of a single crystal of the relaxor ferroelectric $PbMg_{1/3}Nb_{2/3}O_3$. DAFS measurements were performed at the Nb K edge on a half-order Bragg reflection originating from the 1:1 ordered nanodomains. DAFS data analysis provided us with the local structure around Nb atoms in the ordered nanodomains. The Nb-O distance in the ordered region was determined to be 0.052(10) Å shorter than half the lattice parameter of the bulk crystal, in good agreement with one model of the ferroelectric phase transition broadening [JETP **84**, 994 (1997)].

INTRODUCTION

Compositional and structural fluctuations of the "relaxor" ferroelectric $PbMg_{1/3}Nb_{2/3}O_3$, or PMN, have been the focus of ongoing investigation since the first report of its synthesis in 1958 [1]. In addition to strong disorder of the Pb atomic positions at the A site of this ABO_3 cubic perovskite structure, the mixture of Mg^{2+} and Nb^{5+} cations at the B site have made precise structure determination complicated. Transmission electron microscopy [2] and polarized Raman spectroscopy [3] experiments have shown the existence of small, chemically ordered nanodomains. Recently, the structure and size of the ordered nanodomains in single crystal PMN have been refined by Fanning and Robinson (FR) [4]. They carried out

1) *Mailing address*: Building 510 E, Brookhaven National Laboratory, Upton, NY 11973. *Electronic address*: frenkel@bnl.gov. Supported by the DOE grant DEFG02-96ER45439.
2) Partially supported by a National Research Council and by the office of Naval Research.

synchrotron x-ray diffraction measurements of superstructure reflections originating from the ordered regions and measured the nanodomains to be approximately 50 Å in size.

Ordered nanodomains play an important role in several models of the diffuse paraelectric-ferroelectric phase transition in relaxor ferroelectrics [5–7]. The importance of the charge on the B-site for ordering through electrostatic forces in the $A(B'B'')O_3$ ordered regions has been emphasized by Setter and Cross [6] who used $PbSc_{0.5}Ta_{0.5}O_3$ as an example. Comparison between Mg^{2+} and Nb^{5+} ionic radii suggests that Nb-O bonds should be shorter than Mg-O bonds in these ordered domains. The Nb-O bond length is an important parameter which characterizes the charge transfer between MgO_6 and NbO_6 octahedra, since the shorter Nb-O bonds should be more covalent than the longer Mg-O bonds [8].

Bokov [9] demonstrated that the permittivity broadening parameter σ of the ferroelectric phase transition in relaxor ferroelectrics is proportional to the b/a ratio, where b is the displacement of oxygens from their basal planes defined by Pb atoms, and a is the lattice parameter. The coefficient of proportionality is calculated from the model to be 2409 K for PMN [9]. Using ionic radii to calculate b/a in PMN (0.0102), Bokov obtained that the corresponding broadening σ is 25 K, in a relatively good agreement with the experimentally measured 30 K broadening of the transition range in the PMN [10].

To check these and other models of the ferroelectricity in PMN and related perovskites more experimental structural data is needed. As of now, direct measurements of the Nb-O bond lengths in the ordered regions have not been available.

Several attempts have been undertaken to obtain the Nb-O bond length in the ordered regions. FR used the Nb-O distance as a fitting parameter in the refinement of their X-ray diffraction data. Their best fit required the shortening of Nb-O bonds by 0.044(3) Å relative to half of the lattice parameter $a = 4.04$ Å of PMN.

An Extended X-ray Absorption Fine-Structure (EXAFS) experiment has been reported at Nb K edge [8]. EXAFS is a local structure probe, but in the case of PMN the data analysis is complicated by the coexistence of two types of local environments around Nb atoms. Assuming that the local structure in the Nb-rich host is rhombohedrally distorted, Prouzet, et al., [8] however, were able to demonstrate the indirect effect of the short Nb-O bond by an observed increase, from 3 to 4, in the average number per atom of short Nb-O bonds in the PMN.

In the present paper, we report a direct measurement of the local structure around the Nb atom in the ordered nanodomains of a single crystal of $PbMg_{1/3}Nb_{2/3}O_3$ by Diffraction Anomalous Fine Structure (DAFS) [11,12]. DAFS is a relatively new structural technique which combines the short-range structural sensitivity of EXAFS spectroscopy with structural specificity of X-ray diffraction. When measured at the superstructure peak, the DAFS signal contains only the contributions from the ordered nanodomains.

SAMPLE PREPARATION AND DAFS EXPERIMENT

A crystal of pure PMN of roughly 2 mm per side with well formed $\langle 100 \rangle$ faces on three sides was used. Details on the crystal growth can be found elsewhere [4]. X-ray diffraction data were measured using a custom-designed 4-circle Kappa diffractometer at the National Synchrotron Light Source at Brookhaven National Laboratory, beamline X16-C. The orientation matrix of the crystal was determined by measuring several bulk Bragg reflections. DAFS measurements of the (0.5, 2.5, 2.5) Bragg peak were taken from 200 eV below to 600 eV above the Nb K edge energy (18986 eV). The program SUPER was used for data collection, after suitable modification for energy-dispersive measurements. A total of 20 scans were taken which were later averaged for better signal/noise ratio. Fluorescence background was measured by repeating the DAFS scan after moving the 2Θ arm of the diffractometer to an off-peak position.

REDUCING THE DAFS SIGNAL FROM THE BRAGG INTENSITY

The complex DAFS fine-structure function $\chi(E) = \chi'(E) + i\chi''(E)$, which ultimately contains the information about the local structure around the resonant atom, is related to the experimentally measured Bragg peak intensity *via* the anomalous scattering amplitude:

$$\Delta f(E) = f'(E) + if''(E) = f'_a(E) + if''_a(E) + f''_c\left[\chi'(E) + i\chi''(E)\right], \tag{1}$$

where E is the x-ray photon energy, f'_a and f''_a are the atomic parts of f' and f'', respectively, and $f''_c(k)$ is the part of $f''_a(k)$ due solely to the excited core electron [13].

The fine-structure background removal and normalization procedure is formally described by

$$\chi''(k) = \frac{f''(k) - f''_a(k)}{f''_c(k)}, \tag{2}$$

where $k = \sqrt{2m(E - E_0)}/\hbar$ is the photoelectron wave number, E_0 is the x-ray photon energy corresponding to the resonant atom absorption edge.

Equation (2) is the diffraction analog of the standard background removal and normalization procedure for EXAFS. In EXAFS experiments, the fine-structure $\chi(E)$ function is simply related to the experimentally measured total absorption cross-section $\sigma(E)$ through the mass absorption coefficient $\mu(E) \propto \sigma(E)$ with

$$\chi(k) = \frac{\mu(k) - \mu_0(k)}{\mu_0(k)}, \tag{3}$$

where $\mu_0(k)$ is a smooth background function. The methods of determining $\mu_0(k)$ and of analyzing the structural content of $\chi(k)$ are well developed and have been described in detail in several places [14–16]. For DAFS collected in the σ-scattering geometry, with the x-ray polarization vector normal to the scattering plane, the DAFS $\chi''(k)$ and EXAFS $\chi(k)$ are identical. To obtain $\chi(k)$, EXAFS background removal can be applied to $\mu(E) \propto f''(E)/E$, and the fine-structure analysis follows the same procedures.

The DAFS $\chi''(k)$ is not simply related to the experimentally measured Bragg peak intensity $I(\mathbf{Q}, E)$. In the kinematic approximation, the intensity is proportional to the squared amplitude of the crystallographic structure factor $I(\mathbf{Q}, E) \propto |F(\mathbf{Q}, E)|^2$, with

$$F(\mathbf{Q}, E) = \sum_j \left[f_0(Q) + \Delta f(E)\right] e^{i\mathbf{Q}\cdot\mathbf{R}_j} e^{-M_j}, \tag{4}$$

where the sum j is over every atom in the unit cell, with position $\mathbf{R}_j$ and Debye-Waller factor M_j. Isolation of $\chi(k)$ from $I(\mathbf{Q}, E)$ can be accomplished in two ways: 1) spline subtraction and normalization, which leaves a $\mathbf{Q}$-dependent phase residue and amplitude correction in the photoelectron scattering paths [17,18], and 2) iterative Kramers-Krönig decomposition [12,18] of the intensity, which uses the dispersion relations between $f'(E)$ and $f''(E)$ and requires the resonant atom subset of the unit cell to satisfy the symmetry conditions described below. The iterative Kramers-Krönig method was used to isolate $\chi''(E)$ for the analysis presented here.

Since the (0.5, 2.5, 2.5) superstructure peak corresponds to the 1:1 B':B" ordering in the nanodomains where the unit cell size effectively doubles ($a = 8.08$ Å), we can re-define the peak as (1, 5, 5) in terms of a new *Fm3m* unit cell with a composition Pb(8)B'(4)B"(4)O(24) and four formulae in the unit cell. The structure factor corresponding to the photon wavevector $\mathbf{Q} = \frac{2\pi}{a}(1, 5, 5)$ in the new unit cell is equal to $F(E) = 4i\left[f_{\mathrm{B}'}(E) - f_{\mathrm{B}''}(E)\right]$, where $f(E)$ is the scattering amplitude of a single atom (B' or B"). It should be noted that the bulk integer-order Bragg peaks in this experiment were well separated from the superstructure peaks, thus ensuring that the DAFS signal contained contributions from the ordered nanodomains only. In the DAFS analysis for this problem, we make the simplifying assumption that B' = Mg, B" = Nb and, therefore, the local environment is the same for all Nb atoms in the superstructure unit cell. Thus the anomalous amplitude $\Delta f(E)$ and, therefore, DAFS $\chi(E)$ measured on the superstructure peaks can be brought outside the partial structure factor sum over the resonant sites, i.e.,

$$\sum_n \Delta f(E) e^{i\mathbf{Q}\cdot\mathbf{R}_n} e^{-M_n} = \Delta f(E) \sum_n e^{i\mathbf{Q}\cdot\mathbf{R}_n} e^{-M_n} = \Delta f(E)\alpha(\mathbf{Q}), \tag{5}$$

where the sum n is over the Nb atoms only. The *Fm3m* symmetry condition eliminates cross-terms between $f'(E)$ and $f''(E)$ in the intensity, and allows $I(\mathbf{Q}, E)$ to be solved as a simple quadratic equation in $f'(E)$ or $f''(E)$. The remaining part of the structure factor

$$F_0(\mathbf{Q},E) \approx |F_0(\mathbf{Q})|e^{i\Phi_0(\mathbf{Q})} \tag{6}$$

includes the Thomson scattering from all of the atoms in the unit cell, and the anomalous scattering terms from all of the off-resonance electrons. The iterative Kramers-Krönig method can be used only when the coefficient $\alpha(\mathbf{Q})$ is either pure real or pure imaginary. For the (1, 5, 5) superstructure reflection, $\alpha(\mathbf{Q})$ is pure imaginary, and the intensity can be written in a convenient form for computer modeling:

$$I(\mathbf{Q},E) = I_0\left[(\cos\Phi_0 - \beta(\mathbf{Q})f''(E))^2 + (\sin\Phi_0 + \beta(\mathbf{Q})f'(E))^2\right] + I_{\text{offset}}, \tag{7}$$

where $\beta(\mathbf{Q}) = \alpha/|F_0|^2$, and I_0, Φ_0, β and I_{offset} can be used as adjustable fitting parameters in a non-linear least-squares fit to the measured intensity. Since the average structure factor is known, however, Φ_0 and β were held fixed and only I_0 and a linear offset (introduced to correct for neglecting smooth energy dependence in Eq. (6)) $I_{\text{offset}} = a_1 + a_2E$ were allowed to vary.

The data were first corrected for the Lorentz-polarization factor and for self-absorption by the sample. The energy dependent Lorentz-polarization correction for σ scattering is $(E^3\sin 2\theta)^{-1}$ at the Bragg angle 2θ. The self-absorption correction $1/2\mu(E)$ contains absorption fine-structure not only from the domains contributing to the Bragg peak, but from all of the resonant atoms in the diffracting volume [19]. Fluorescence EXAFS measured simultaneously with the DAFS was used for the self-absorption correction.

The iterative Kramers-Krönig procedure was applied to fit Eq. (7) to the experimental DAFS data and to extract f' and f'' using computer programs developed at the University of Washington [18].

Bare-atom $\Delta f_a(E)$ calculated using the method of Cromer-Liberman [20] were used for the initial guess to $\Delta f(E)$. The normalized DAFS data $I(E) = (I_{\text{signal}} - I_{\text{bkg}})/I_0)$, where I_{signal} is the total Bragg intensity, I_{bkg} is the fluorescence background, and I_0 is the incident beam monitor signal, are shown in Fig. 1. The resulting $f'(E)$ and $f''(E)$ are shown in Fig. 2. The calculated absorption cross-section $\sigma(E)$ is shown in Fig. 3.

DATA ANALYSIS AND RESULTS

The anomalous scattering amplitude $f''(E)$ obtained by the method described above was converted to the mass absorption coefficient $\mu(E)$ and analyzed using the UWXAFS [21] data analysis package. In accordance with Eq. (3), smooth atomic background (Fig. 3) was removed from $\mu(E)$ using computer program AUTOBK [16], and EXAFS signal $\chi(k)$ was obtained (Fig. 4 (a)). Due to the significant amount of noise in the $\chi(k)$ data above 8 Å^{-1}, we analyzed the Nb-O (1NN) distances only.

The theoretical EXAFS equation for the single scattering contributions can be expressed in the form [14]:

$$\chi(k) = \frac{S_0^2 N}{kr^2} f(k) e^{-2k^2\sigma^2} \sin(2kr + \delta(k)) e^{-2r/\lambda(k)}, \tag{8}$$

where S_0^2 is the passive electron amplitude reduction factor, N is the coordination number of the Nb-O bonds (6), r is half the total scattering path length, σ^2 is the mean square relative deviation of r, $f(k)$ and $\delta(k)$ are the effective scattering amplitude and phase shift, respectively, and $\lambda(k)$ is the photoelectron mean free path.

$f(k)$, $\delta(k)$ and $\lambda(k)$ for Nb-O bonds were calculated with an *ab initio* FEFF6 [22] code using the cubic perovskite structure of the $Fm3m$ space group with $a = 8.08$ Å as a model. Small deviations of the 1NN distances from this model structure by less than 0.1 Å should not affect $f(k)$, $\delta(k)$, and $\lambda(k)$ by more than 5%, which is

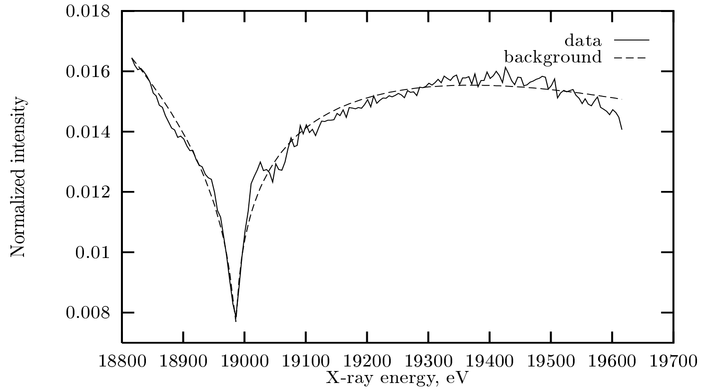

FIGURE 1. Normalized DAFS signal (solid) and a smooth background (dash) obtained with Eq. (7).

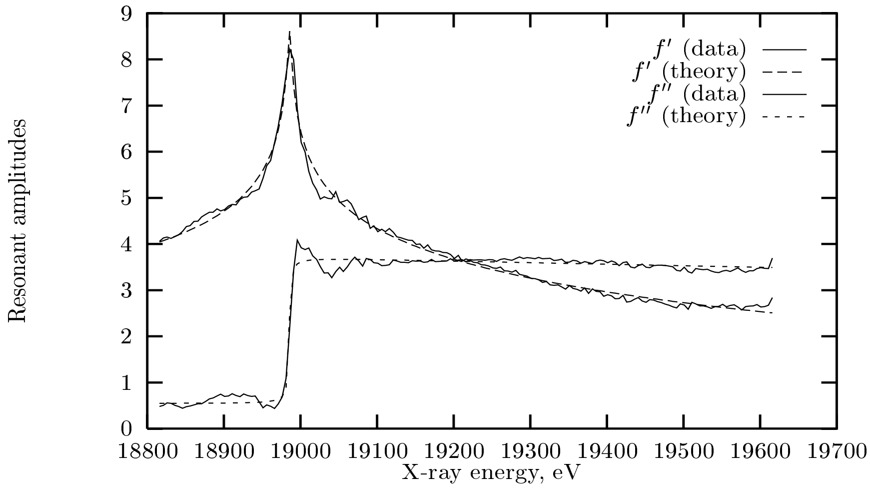

FIGURE 2. The results for the $f'(E)$ and $f''(E)$ (solid) as obtained by fit with the Kramers-Krönig iterative procedure. Theoretical bare atom response functions $f_a'(E)$ and $f_a''(E)$ (dash), used as a starting approximation, are shown for comparison.

comparable to the systematic error in FEFF6 theory.

The non-linear least squares fit was performed in r space by Fourier transforming the data and theory within the δk range between 2 and 7 Å. The data and theory were k-weighted before the transforms. The fitting range in r space δr was between 1.1 and 2.2 Å giving 5 relevant independent data points N_{idp}, according to the definition [23]: $N_{\text{idp}} = 2\delta k \delta r/\pi + 2$. The number P of fitting parameters, therefore, should not exceed 5.

We varied 3 parameters in Eq. (8) to account for possible deviations of the local structure from the model. These variables were: correction to the photoelectron energy origin, ΔE_0, and the two leading cumulants of the Nb-O effective pair distribution function, i.e., correction to the model distances (Δr) and a mean square disorder in the bond lengths (σ^2). To decrease the number of variables, we fixed S_0^2 to be equal 0.9 as found previously in the Nb K edge EXAFS analysis of $KNbO_3$ [24]. An anharmonic correction to the phase of $\chi(k)$, the third cumulant $\sigma^{(3)}$, was not used in our fit procedure. Although this factor is important for the correct distance determination, all our attempts to add it to the fit resulted in unreasonably large values for Δr and ΔE_0, because of their correlation with $\sigma^{(3)}$. Previous works demonstrated that the effect of anharmonicity for B-O bonds in ABO_3 oxygen perovskites is negligible since they are characterized by the relatively rigid oxygen octahedra, therefore we believe that neglecting the anharmonic correction is a good approximation.

The Nb-O distance in the ordered region was determined to be 1.968(10) Å, i.e., 0.052(10) Å shorter than half the lattice parameter (4.04 Å) of the PMN. This result is in good agreement with the previous EXAFS [8] and x-ray diffraction [4] results.

The mean square disorder σ^2 in the Nb-O bonds length was determined to be 0.0087(3) Å^2. Prouzet, et al., [8] obtained an average σ^2 of 0.0036 Å^2 by analysis of the bulk EXAFS data. Their result, however, included the contributions of all Nb-O bonds and not just those associated with the 1:1 ordered nanodomains.

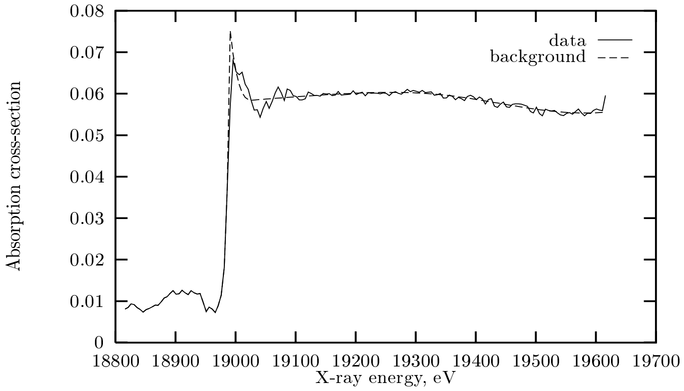

FIGURE 3. Normalized absorption cross-section $\sigma(E)$ (solid) and a smooth background function (dash) obtained with AUTOBK.

DISCUSSION

Our DAFS analysis resulted in the measurement of the Nb-O bond length and its mean square disorder in the ordered region of PMN. We found that this bond is significantly (by 0.052(10) Å) shorter than the average B-O distance in bulk PMN. Our result is an independent measurement in favor of the model suggested by Fanning and Robinson [4] based on their X-ray diffraction analysis of superstructure reflections of PMN. In their model, FR proposed chemical 1:1 ordering of B' and B" atoms, together with concomitant displacements of oxygen atoms towards Nb in a (100) direction. Prouzet, et al. [8], arrived at similar conclusions by analyzing their EXAFS data obtained for the bulk PMN.

Although the DAFS method combines the capabilities of diffraction and EXAFS in a single technique, it has several enhanced sensitivities compared to the separate techniques. First, it can provide EXAFS-like information for the specific subset of

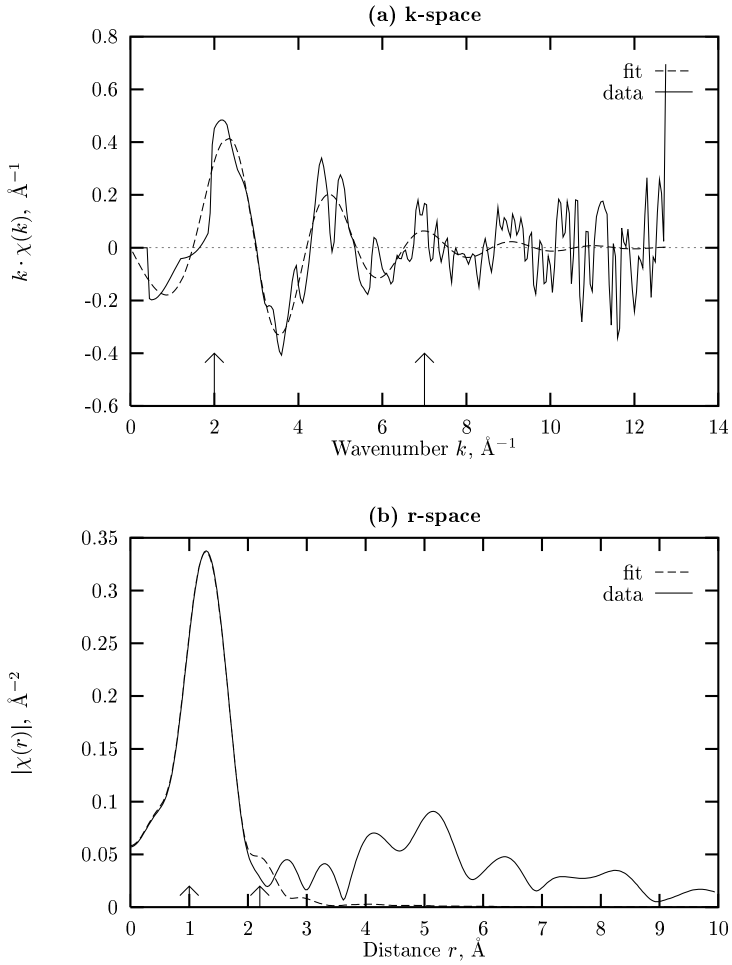

FIGURE 4. Fit of the FEFF6 theory (dash) to the data (solid) in (a) k-space and (b) r-space. Weighting factor k was applied to both theory and data.

atoms selected by the diffraction condition [25]. This makes DAFS clearly advantageous over EXAFS for analysis of PMN. In conventional EXAFS measurement of PMN, the resonant atom resides in both phases, ordered nanodomains and Nb-rich host domains. Therefore, sophisticated, model-dependent analysis is necessary to extract the contribution of the nanodomain structure to the total signal. Using DAFS, we filtered the nanodomain structure out of the total structure factor by aiming the detector at the superstructure reflections, originated from the ordered nanodomains only.

Second, DAFS technique has the same advantage as EXAFS over the diffraction analysis. Since the two former methods contain the phase information of the interference between the outgoing and backscattered photoelectron, their Fourier transforms contain direct information on the local structure in the system. In diffraction techniques, only the intensity of the diffracted wave is measured, and additional modeling is required to determine structural information.

Third, DAFS inherits from EXAFS technique a better spatial resolution over diffraction method. In both EXAFS and diffraction, the spatial resolution is inversely proportional to the upper end of the q range of the data, $1/q_{\max}$. In the case of PMN, due to the small size of coherent scattering region (50 Å) both q and k ranges in the XRD and DAFS experiments, respectively, were limited by small intensity of the superstructure Bragg reflections and the low signal/noise ratio. In both cases, $k_{\max}$ was approximately 7 Å^{-1}. For DAFS, however, this translates to a spatial resolution by a factor of two better than that of the diffraction measurement since the momentum transfer in DAFS (and EXAFS) experiments is $q = 2k$. Even with this enhanced resolution, however, due to the small nanodomain size and, therefore, limited amount of information in the DAFS data, we were unable to unambiguously resolve subtle details of the Nb local environment beyond the first Nb-O shell. We were unable to determine whether the equilibrium positions of Nb atoms are in the center of symmetry of the oxygen octahedron, or displaced in one of 8 possible $\langle 111 \rangle$ directions.

Our results for the Nb-O distance shortening from its bulk value by 0.052(10) Å, and the corresponding ratio of this displacement to the bulk lattice parameter, $b/a = 0.013(2)$, allow us to calculate a broadening parameter σ for the ferroelectric phase transition. Following the model proposed by Bokov [9], we obtain for PMN: $\sigma = 2904 \times 0.013 = 31 \pm 6$ K. This result is in very good agreement with the experimental broadening of 30 K [10].

Recent experiments with La-doped PMN crystals showed an increase in the size of the nanodomains up to 1000 Å [4]. This presents more opportunities for further investigation of the local structure in the ordered regions. For example, analysis of Nb-Pb bonds would help solve the long lasting controversy between the models of disorder of Pb atoms. Multiple-scattering analysis of Nb-O-Mg distances promises more information about charge transfer between NbO_6 and MgO_6 octahedra.

CONCLUSIONS

Shortening by 0.052(10) Å of Nb-O bonds in NbO_6 octahedra in the ordered nanodomains of $PbMg_{1/3}Nb_{2/3}O_3$ relative to the average Nb-O distance has been established by DAFS. This result is in good agreement with previous results obtained by XRD and EXAFS methods, and with the experimentally observed broadening of the ferroelectric phase transition.

REFERENCES

1. Smolenskii G. A. and Agranovskaya A. I., *Sov. Phys. – Tech. Phys.* **3**, 1380 (1958).
2. Randall C., Bhalla A., Shrout T., and Cross L. E., *J. Mater. Res.* **5**, 829 (1990).
3. Siny I. and Boulesteix C., *Ferroelectrics* **96**, 119 (1989).
4. Fanning D. M. and Robinson I. K., to be published.
5. Galasso F. S., *Structure, Properties and Preparation of Perovskite-Type Compounds,* Paris: Pergamon Press, 1969.
6. Setter N. and Cross L. E., *J. Mat. Science* **15**, 2478 (1980).
7. Randall C. A., Barber D. J., Whatmore R. W., and Groves P., *J. Mat. Science* **21**, 4456 (1986).
8. Prouzet E., Husson E., de Mathan N., and Morell A., *J. Phys.: Condens. Matter* **5**, 4889 (1993).
9. Bokov A. A., *JETP* **84**, 994 (1997).
10. Smolenskij G. A., Bokov V. A., Isupov V. A., *et al., Physics of Ferroelectric Phenomena* [in Russian], Leningrad: Nauka, 1985.
11. Stragier H., Cross J. O., Rehr J. J., Sorensen L. B., Bouldin C. E., and Woicik J. C., *Phys. Rev. Lett.,* **69**, 3064 (1992).
12. Pickering I. J., Sansone M., Marsch J., and George G. N., *J. Am. Chem. Soc.,* **115**, 6203 (1993).
13. Cross J. O., Newville M., Rehr J. J., Sorensen L. B., Watson G., Bouldin C. E., Bell M. I., Gouder T., and Lander G. H., unpublished.
14. Stern E. A. and Heald S. M., *Handbook on Synchrotron Radiation*, edited by E. E. Koch; New York: North-Holland, 1983, Ch. 10.
15. Koningsberger D. C. and Prins R., editors, *X-Ray Absorption: Principles, Applications, Techniques of EXAFS, SEXAFS, and XANES*, Vol. 92 of *Chemical Analysis*; New York: John Wiley & Sons, 1988.
16. Newville M., Livinš P., Yacoby Y., Rehr J. J., and Stern E. A., *Phys. Rev. B* **47**, 14126 (1993).
17. Arčon I. and Hribar M., *X-Ray Absorption Fine Structure*, edited by S. S. Hasnain; London: Ellis Horwood, 1991, pp. 726-728.
18. Cross J. O., Ph.D. Thesis, University of Washington, 1996.
19. Cullity B. D., *Elements of X-Ray Diffraction*, 2nd edition, Addison-Wesley, 1978, Ch. 4.
20. Cromer D. T. and Liberman D., *J. Chem. Phys.,* **53**, 1891 (1970).

21. Stern E. A., Newville M., Ravel B., Yacoby Y., and Haskel D., *Physica B,* **208 & 209**, 117 (1995).
22. Zabinsky S. I., Rehr J. J., Ankoudinov A., Albers R. C., and Eller M. J., *Phys. Rev. B* **52**, 2995 (1995).
23. Stern E. A., *Phys. Rev. B* **48**, 9825 (1993).
24. Frenkel A. I., Wang F. M., Kelly S., Ingalls R., Haskel D., and Stern E. A., *Phys. Rev. B* **56**, 10869 (1997).
25. Sorensen L. B., Cross J. O., Newville M., Ravel B., Rehr J. J., Stragier H., Bouldin C. E., and Woicik J. C., *Resonant Anomalous X-Ray Scattering*, edited by Materlik G., Sparks C. J., and Fischer K.; Amsterdam, Elsevier Science, 1994, p. 389.
26. You H. and Zhang Q. M., *Phys. Rev. Lett.,* **79**, 3951 (1997).